

Supporting Information for

Waste-to-wealth: atomically dispersed cobalt-nitrogen-carbon from spent LiCoO₂

Miaosen Yang,^a Yanhui Sun,^{a,b} Shuhan Lv,^c Tian Zhang,^{a,b} Lei Yang,^d Zongge Li,^b and Guoxin Zhang^{b,*}

a. School of Chemical Engineering, Northeast Electric Power University, Jilin, Jilin 132012, China.

b. Al-ion Battery Research Center, College of Energy Storage Technology, Shandong University of Science and Technology, Qingdao, Shandong 266590, China. Email: zhanggx@sdust.edu.cn

c. Beijing 21st Century International School, Beijing 100089, China

d. Research Center for Intelligent and Wearable Technology, College of Textiles and Clothing, Qingdao University, Qingdao, Shandong 266071, China

1. Experimental Section

1.1 Chemicals and reagents

Lithium cobalt oxide (LiCoO_2) was provided by a battery recycling company. Formamide (CH_3NO , purity >99%) was bought from Tianjin Damao Chemical Factory. ZnO (99.8%, 50 ± 10 nm), $\text{In}(\text{OH})_3$ (99% purity), Na_2SnO_3 (A.R. grade) were purchased from Aladdin Co., Ltd. KOH (95%) was bought from Shanghai Macklin Biochemical Co., Ltd. Absolute ethanol was purchased from Sinopharm Chemical Reagent Co., Ltd. Nafion solution (5.0 wt%, Dupont) and commercial Pt/C (20.0 wt.%) were bought from Shanghai Hesun Electric Co., Ltd. Carbon black (BP2000) was purchased from Nanjing Xianfeng Nanomaterial Technology Co., Ltd. All reagents were used as received without further purification.

1.2 Preparation of atomically dispersed Co-NC from spent LiCoO_2

Typically, a mixture of 0.2 g LiCoO_2 , 1.0 g ZnO, and 40.0 mL formamide was placed into a 50 mL-packed ZrO_2 jar and ball milled at 300 Hz for 2 h. The resulting white slurry was then solvothermal-treated at 180 °C for 12 h. The autoclave was allowed naturally cooling down to room temperature before opening the vessel. Subsequently, the as-obtained black, named CoZn-NC180, was thoroughly washed 2-3 times with anhydrous ethanol and dried at 60°C in a vacuum overnight. The dried CoZn-NC180 was then ground in a mortar and heated at 950°C under N_2 protection for 1 hour with a ramp of 5°C min^{-1} . Control sample of Zn-NC950 was synthesized by excluding the addition of LiCoO_2 , the rest steps were following the synthesis of Co-NC950.

1.3. Materials characterizations

Powder X-ray diffraction (XRD) was carried out on a Brüker D8 Advance diffractometer using $\text{Cu K}\alpha$ radiation ($\lambda = 0.15406$ nm) at 40 kV and 40 mA. Scanning electron microscopy (SEM) was carried out on an Apreo S HiVac scanning electron microscope at an accelerating voltage of 15 kV. Transmission electron microscopy

(TEM), high-resolution TEM (HRTEM) images, and high angle annular dark-field scanning transmission electron microscopy (HAADF-STEM) images were obtained with an FEI Talos 200S high-resolution transmission electron microscope at an accelerating voltage of 200 kV. Raman spectra were obtained by a DXR2 Raman microscope (Thermo Fisher) using a 532 nm argon laser line as the excitation source. Brunauer-Emmett-Teller (BET) N₂ adsorption-desorption isotherms were performed on a Micromeritics-ASAP2460 to obtain the specific surface area (SSA) of all samples at 77 K, degassed at 300°C before measurement. The pore size distribution maps were determined by using the density functional theory (DFT) method. Thermogravimetric analysis (TGA, STA449F5) was operated under an N₂/O₂ atmosphere with a heating rate of 5 °C min⁻¹. X-ray photoelectron spectroscopy (XPS) analysis was carried out on a PHI 5000 Versaprobe system, using monochromatic Al K α radiation (1486.6 eV). All binding energies were referenced to the C 1s peak at 284.6 eV. X-ray absorption spectra (XAS) were collected on the BL01C1 beamline of the NSRRC. The radiation was monochromatic by a Si (111) bicrystal monochromator. Cobalt *k*-edge XANES data for Co-NC were recorded in fluorescence mode, while the references (Co foil, Co₃O₄, CoO, and CoPc) were recorded in transmission mode. Reduction and analysis of XANES and EXAFS data were processed by Athena software. The K³-weighted EXAFS spectra in the range of 3-10.0 Å⁻¹ in K-space were Fourier transformed to give a radial distribution function.

1.4 Electrochemical measurements

The ORR measurements were carried out at room temperature on a typical three-electrode system using a CHI-760e electrochemical workstation (Shanghai Chenhua). A glassy carbon electrode (GCE), a saturated glycerol electrode (SCE), and a graphite rod electrode were used as the working, reference, and counter electrodes, respectively. The catalyst ink was prepared by ultrasonically mixing 5.0 mg catalyst, 1.0 mg carbon black and 10.0 μ L Nafion solution (5.0 wt%) in 500 μ L absolute ethanol. The dispersed catalyst ink was then casted onto a glassy carbon rotating ring disc electrode (RRDE) with a loading of approximately 0.25 mg cm² for all measured samples. The aqueous

0.1 mol L⁻¹ KOH solution was used as the electrolyte. O₂ gas was blowing into the electrolyte for at least 30 minutes before ORR measurements to reach O₂ saturation. Before collecting data, all the working electrodes were pre-treated by repeated cyclic voltammetry scans at a rate of 100 mV s⁻¹ to fully activate the accessible surface of electrodes. Linear sweep voltammetry (LSV) polarization curves were obtained in a 0.1 mol L⁻¹ KOH electrolyte at a scan rate of 5.0 mV s⁻¹ at 1600 rpm. ORR stability was determined by the chronoamperometric technique (*i*-*t*) at 0.4 V vs RHE. All the potentials were converted to the reversible hydrogen electrode (RHE) according to equation (1).

$$E(\text{RHE}) = E(\text{SCE}) + 0.241 \text{ V} + 0.059 \text{ V} \times \text{pH} \quad (1)$$

ORR polarization curves for calculating the transfer electron number (*n*) and hydrogen peroxide yield (H₂O₂%) were collected at a rotation rate of 1600 rpm and a scan rate of 5.0 mV s⁻¹. The hydrogen peroxide yield (H₂O₂%) and the number of electrons transferred (*n*) were determined by the following equations.¹

$$\text{H}_2\text{O}_2\% = 200 \times \frac{I_r/N}{I_d + I_r/N} \quad (2)$$

$$n = 4 \times \frac{I_d}{I_d + I_r/N} \quad (3)$$

where *I_d* is the disc current and *I_r* is the ring current, the platinum ring has a current collection efficiency (*N*) of 0.37.

1.5 Al-air battery (AlAB) measurements

The Al-air battery measurements were carried out on a homemade electrochemical cell with a sandwich structure. Typically, to assemble a gas diffusion electrode (GDE), 5.0 mg catalyst was initially dispersed into a mixed solution of 500 μL ethanol and 10.0 μL 5.0 wt% Nafion to prepare catalyst ink. The resulting catalyst is then coated onto conductive carbon paper to achieve a loading mass of 1.0 mg cm⁻² and the gas diffusion

area is controlled to 1.0 cm^2 . A polished 0.8 mm thick Al plate is used as the anode. The electrolyte was 6.0 M KOH containing additives of Na_2SnO_3 , $\text{In}(\text{OH})_3$, and ZnO .² The power density was obtained by testing the discharge curve on a CHI-760E electrochemical workstation. The rate performance of the AlAB was evaluated by performing electrostatic discharges at different current densities: 1.0, 5.0, 10.0, 20.0, and 50.0 mA cm^{-2} . The stability and reusability of catalysts were also verified by performing mechanical recharging, *i.e.*, replacing the Al anode after the battery ending.

2. Supplementary Figures

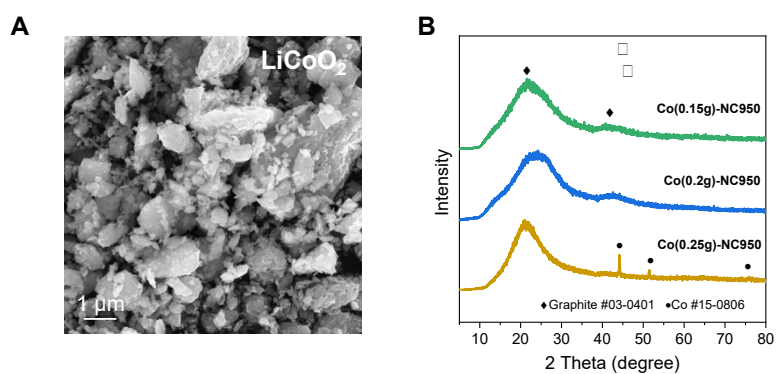


Figure S1. (A) SEM of LiCoO_2 . (B) XRD of Co-NC950 with different LiCoO_2 usage.

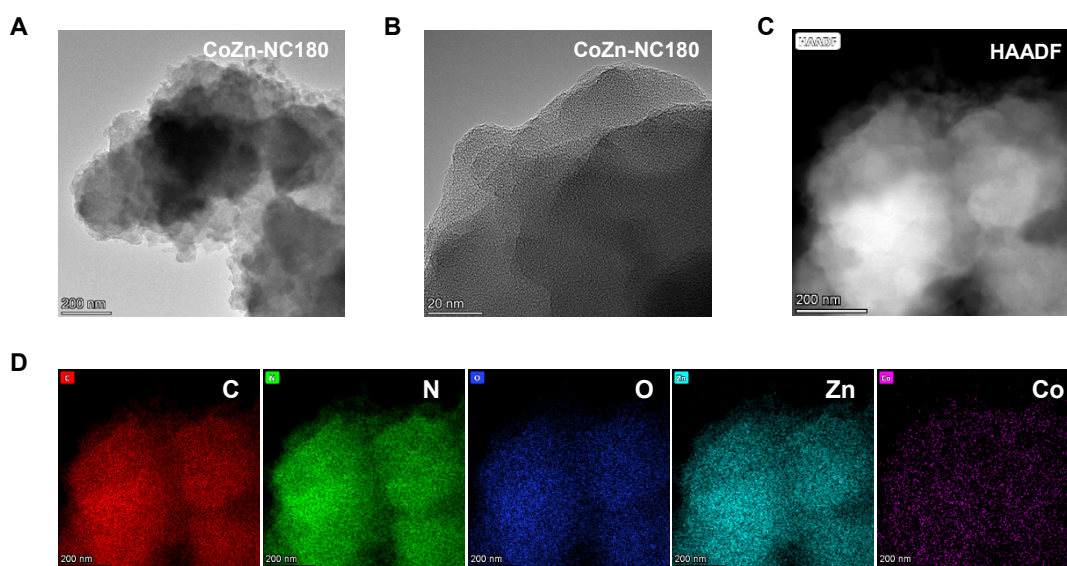


Figure S2. (A) TEM, (B) HRTEM, and (C) HAADF-STEM image, and (D) EDS mapping images of CoZn-NC180.

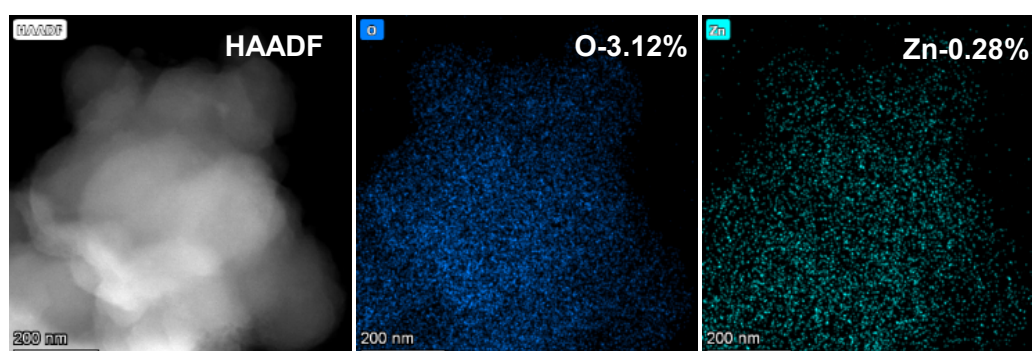


Figure S3. HAADF-STEM image, and EDS mapping images of Co-NC950.

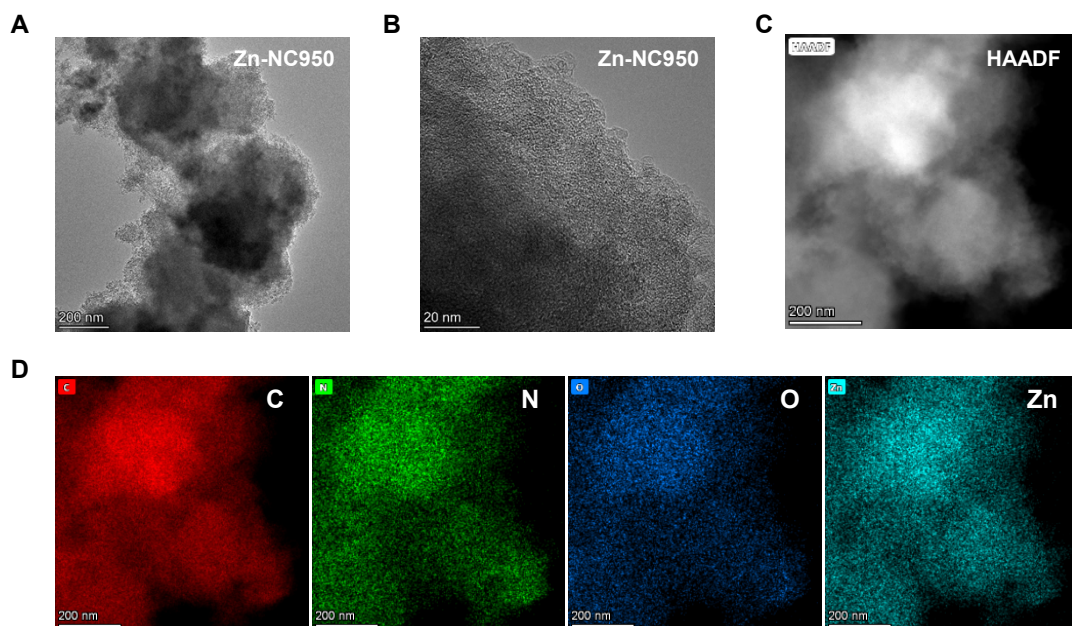


Figure S4. (A) TEM, (B) HRTEM, and (C) HAADF-STEM image, and (D) EDS mapping images of Zn-NC950.

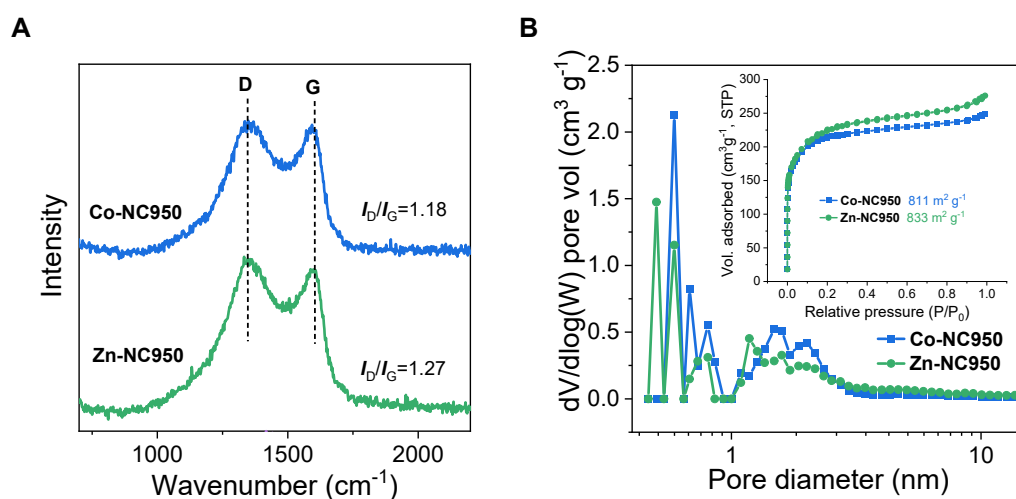


Figure S5. (A) Raman spectra of Co-NC950 compared to those of Zn-NC950, CoZn-NC180 and LiCoO₂. (B) BET measurements of Co-NC950 and Zn-NC950: N₂ isotherms and pore distribution curves.

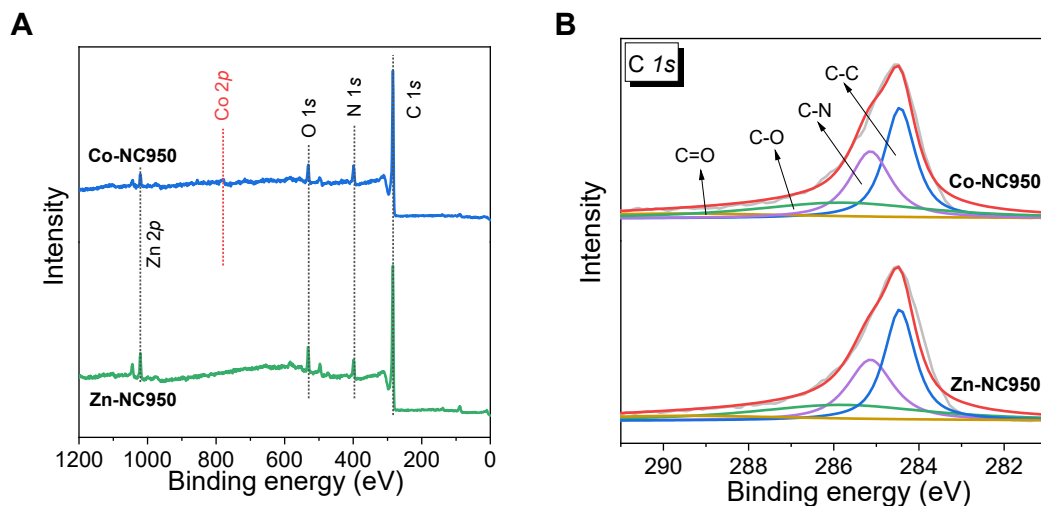


Figure S6. X-ray photoelectron spectroscopy (XPS) characterizations of Co-NC950 and Zn-NC950: (A) element survey, (B) C1s spectra.

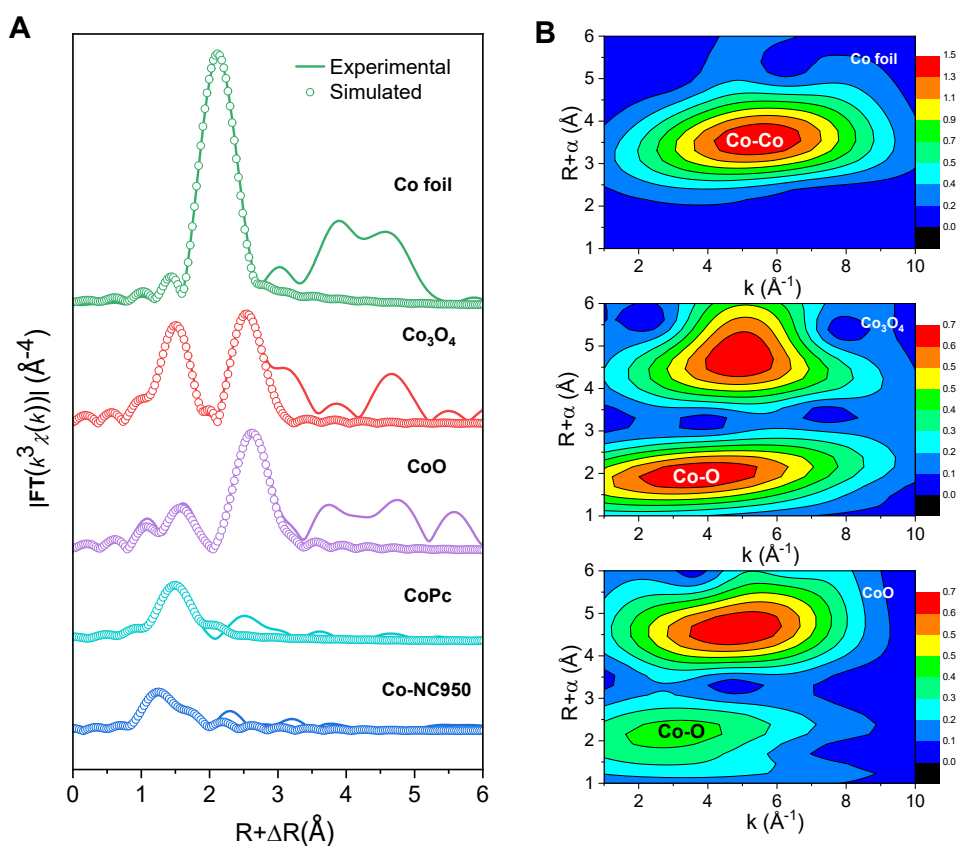


Figure S7. (A) Fourier transformed (FT) k^3 -weighted $\chi(k)$ -function of the EXAFS spectra for the Co K-edge of Co-NC950 and its references, the corresponding Co K-edge EXAFS fitting curves of Co-NC950 and its references, were also provided. (B) Wavelet transformed (WT) EXAFS of Co foil, Co_3O_4 , and CoO.

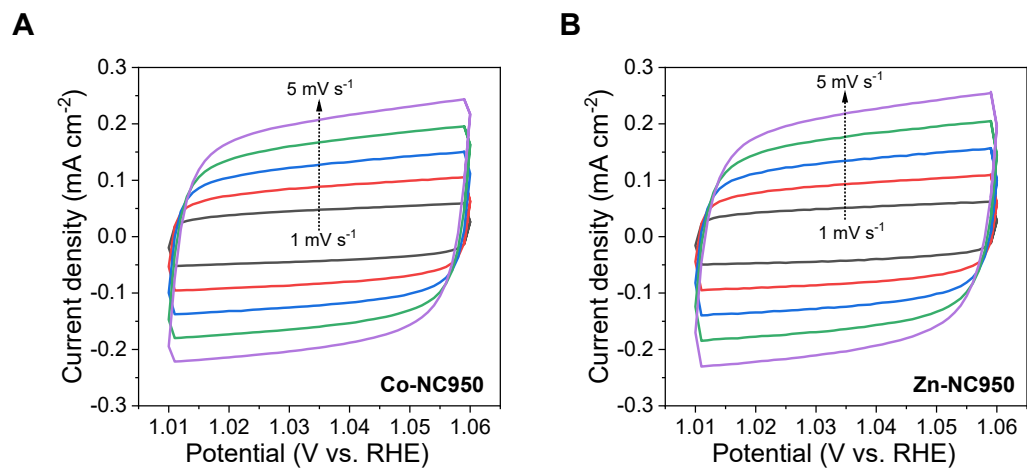


Figure S8. CV profiles of (A) Co-NC950 and (B) Zn-NC950 with a potential range of 1.01 to 1.06 V vs. RHE.

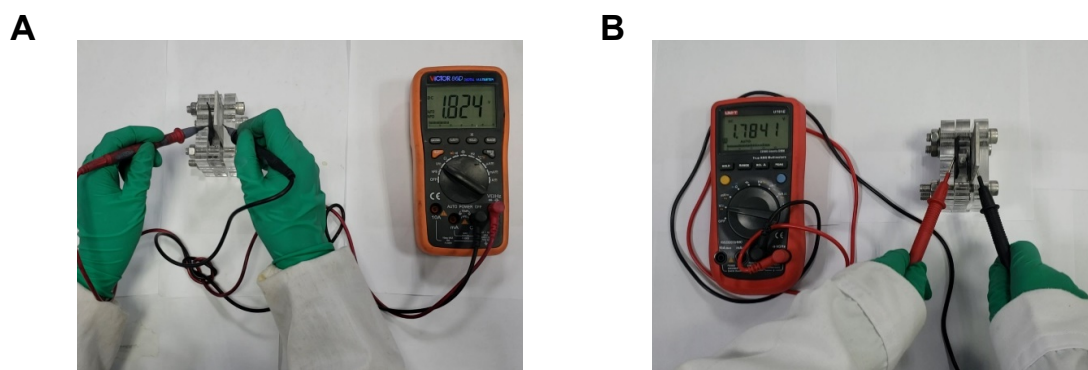


Figure S9. Photograph of the open circuit voltage of AAB assembled with (A) Co-NC950, (B) Pt/C.

3. Supplementary Tables

Table S1. XPS and ICP element analysis of Co-NC950 and Zn-NC950.

Sample	at%C	at%N	at%O	at%Zn	at%Co	ICP-Co wt%	ICP-Zn wt%
Co-NC950	82.62	8.95	6.16	0.85	1.42	2.31	1.06
Zn-NC950	80.35	9.30	8.04	2.31	/	/	4.16

Table S2. EXAFS fitting results of Co-NC950.

Sample	Shell	N ^a	R(Å) ^b	$\sigma^2(\text{Å}^2)$ ^c	ΔE_0 (eV) ^d	R factor
Co foil	Co-Co	9.83	2.49	0.0062	-1.82	0.0046
CoO	Co-O	6.09	2.11	0.0117	4.79	0.0109
	Co-Co	4.79	3.10	0.0103	-5.23	
Co₃O₄	Co-O	4.30	1.92	0.0030	4.05	0.0054
	Co-Co	9.32	2.91	0.0102	8.41	
CoPc	Co-N	4.06	1.91	0.0032	4.36	0.0073
Co-NC950	Co-N	4.25	1.92	0.0190	4.93	0.0125

^a N: coordination numbers; ^b R: bond distance; ^c σ^2 : Debye-Waller factors; ^d ΔE_0 : the inner potential correction. R factor: goodness of fit.

4. Supplementary References

1. Sun, Y.; Li, Z.; Wu, Y.; Tian, J.; Wang, Y.; Yang, M.; Zhang, G., Formamide-soluble solid-state ZnO as Zn source for synthesizing FeCo-NC with ultrahigh oxygen reduction reaction activity. *Mater. Chem. Front.* **2022**, *6* (1), 78-85.
2. Nie, Y.; Gao, J.; Wang, E.; Jiang, L.; An, L.; Wang, X., An effective hybrid organic/inorganic inhibitor for alkaline aluminum-air fuel cells. *Electrochim. Acta* **2017**, *248*, 478-485.